Microwave Imaging—Complex Permittivity Reconstruction by Simulated Annealing

Line Garnero, Ann Franchois, Jean-Paul Hugonin, Christian Pichot, and Nadine Joachimowicz

Abstract—**This paper refers to quantitative reconstruction of the dielectric properties of a strongly inhomogeneous object by means of active microwave imaging. An iterative reconstruction algorithm based on simulated annealing is presented. In some cases, this method seems to be more efficient than iterative deterministic methods and we show that it can converge to an accurate solution when other methods diverge.**

I. Introduction

THE penetration of microwaves in various materials gives active microwave imaging a large potential for applications in domains such as non-destructive testing, civil engineering and medical imaging [1]–[3]. This fairly recent imaging technique is aimed at obtaining some information about the inside of an object exposed to low power incident microwave radiation from external scattered field measurements. It is known that the scattered microwave field is sensitive to the complex permittivity distribution of an object. The complex permittivity is of particular interest in the case of medical imaging, for it depends on the morphology, the blood flow and the temperature of a tissue, hence active microwave imaging is complementary to existing imaging techniques (X-ray tomography, nuclear magnetic resonance, ultrasound, impedance tomography,...). Diffraction effects cannot *a priori* be neglected since the scatterer's dimensions are comparable to the wavelength. The complex permittivity is then related in a nonlinear way to the scattered field, complicating the resolution of the inverse problem.

During the last decade much attention has been paid to the development of reconstruction algorithms. Methods based on diffraction tomography [4]–[7] provide a reconstruction of the polarization current density from which the complex permittivity can be derived in the framework of the Born approximation. They are fast and relatively noise insensitive but their applications are restrained to qualitative or quantitative imaging of weak quasi-homogeneous scatterers and to differential imaging [8]. These limitations have stimulated us to develop iterative methods, which enable injection of *a priori* information, for quantitative reconstruction of highly contrasted objects of practical interest in the medical domain.

We present here a method based on simulated annealing, a stochastic approach which was first used in optimization problems with a large number of variables [9] and then in image reconstruction in nuclear medicine [10]. Theoretically it converges to the global minimum of a cost function while deterministic methods often become trapped in local minima. In Section II we give the theoretical background of the method. First, we treat the forward scattering problem, that is solved in each iteration, and we show that it can be simplified in the case of simulated annealing. The general principles of simulated annealing and the way we applied it to microwave imaging are described. In Section III we present some results obtained with simulated data and compare them to results from a Newton–Kantorovich type deterministic method we recently developed [11]. Results demonstrating a sequential use of the two methods also are presented. In Section IV we give some concluding remarks.

II. Theory and Formulation

We applied the proposed reconstruction algorithm to the limited case of cylindrical objects of arbitrary cross-sectional shape under multi-incidence TM excitation. Fig. 1 illustrates the imaging geometry and notation. The section S of a cylindrical object which may be strongly inhomogeneous is characterized by its complex permittivity $\epsilon^*(r)$:

$$\epsilon^*(r) = \epsilon_0 \epsilon_r(r) + i\sigma(r)/\omega, \tag{1}$$

with $\epsilon_r(r)$ the relative permittivity and $\sigma(r)$ the conductivity at a point $r(x, y)$. It is surrounded by a medium of complex permittivity ϵ^*_{ext}. Note that the dielectric properties do not vary along the cylinder's axis Oz. An incident plane wave of angular frequency ω with electric field E^i polarized parallel to Oz illuminates the object. The scattered field is measured by detectors situated on a line L perpendicular to the propagation direction of the incident wave. This is repeated for different angles θ of the line and of the incident field. The inverse problem then consists of estimating the complex permittivity distribution $\epsilon^*(r)$ of the section from these multi-incidence measurements. As a forward problem is solved for each iteration of the simulated annealing reconstruction algorithm—i.e.,

Manuscript received April 4, 1991; revised July 10, 1991.

L. Garnero and J.-P. Hugonin are with Institut d'Optique. URA 14 CNRS, BP 147, 91403 Orsay, France.

A. Franchois, C. Pichot, and N. Joachimowicz are with Equipe Electromagnétisme, Laboratoire des Signaux et Systemes (CNSRS-ESE), 91192, Gifsur-Yvette Cedex, France.

IEEE Log Number 9102824.

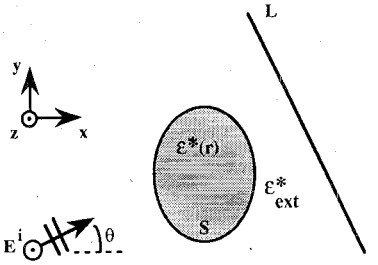

Fig. 1. Geometry for microwave tomography.

calculating the scattered field for a given distribution $\epsilon^*(r)$ and incident field—we will first treat this aspect with more detail.

A. Forward Problem

Let the total electric field at a point r, $E(r)$, be the sum of the incident field $E^i(r)$—i.e., the field if there were no object—and the scattered field $E^s(r)$. These fields are polarized parallel to Oz since the characteristics of the object do not vary along the cylinder's axis, resulting in a reduction of the wave equation to the scalar helmholtz equation for a homogeneous medium with induced sources on the right hand side:

$$\Delta E + k_{\text{ext}}^2 E = \left(k_{\text{ext}}^2 - k^2(r)\right)E, \tag{2}$$

where $k^2(r) = \omega^2 \mu_0 \epsilon^*(r)$. The exact solution of (2) is represented by the integral equation:

$$E(r) = E^i(r) + \iint_S \left(k_{\text{ext}}^2 - k^2(r')\right)E(r')G(r;r')\,dr', \tag{3}$$

where G is the free-space Green's function for a homogeneous medium:

$$G(r;r') = -(i/4)H_0^{(1)}\left(k_{\text{ext}}|r - r'|\right), \tag{4}$$

with $H_0^{(1)}$ the Hankel function of the first kind for a $e^{-i\omega t}$ time dependence.

We used the moment method [13] with pulse basis functions to calculate the total electric field in the section S, discretized into N rectangular cells in this case. The cell size is chosen to be small enough so that the field and complex permittivity can be considered constant in each cell. A system of linear equations of order N is obtained:

$$\left[-\left(k_{\text{ext}}^2 - k^2(r_j)\right)\iint_{S_j} G(r_i;r')\,dr' + \delta_{ij}\right]\begin{bmatrix} E(r_1) \\ \vdots \\ E(r_N) \end{bmatrix} = \begin{bmatrix} E^i(r_1) \\ \vdots \\ E^i(r_N) \end{bmatrix}. \tag{5}$$

The inversion of this system is carried out by a direct Gauss–Jordan algorithm and gives the values of E in the center $r_1, \cdots, r_N$ of each cell of the section. The scattered field on the measurement line is then calculated by means of a discretized version of the integral in (3) with points r located on the line.

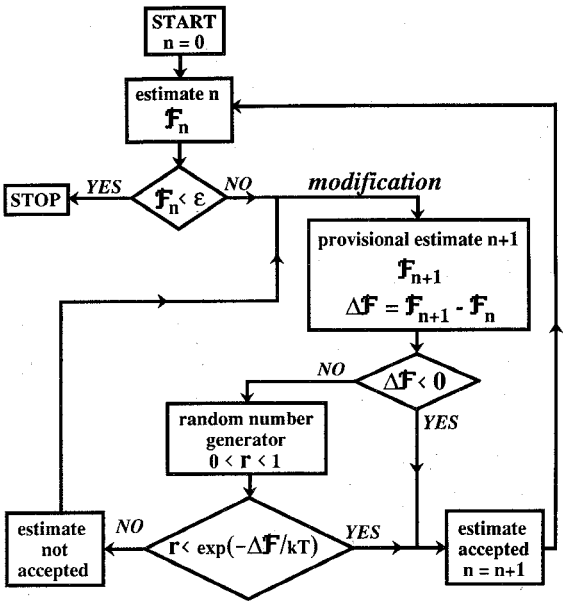

Fig. 2. Scheme of a simulated annealing technique.

B. Simulated Annealing: Principles

The simulated annealing technique (SA) is an optimization algorithm derived from the Metropolis algorithm [14] and has been applied to the optimization of problems where many parameters are involved (circuit design, image reconstruction,...). SA searches for the optimum state of a system, which is defined as the global minimum of a cost function $\mathcal{F}$ of the system. Starting from an arbitrary initial estimate, it introduces in each iteration a slightly modified estimate, for which the cost is calculated. This new estimate is then accepted or rejected. Moving from one estimate to another, it tries to find the global minimum of the cost function in a way similar to the physical annealing process of an amorphous hot solid of high energy cooling towards a monocrystal of minimum energy. The temperature is lowered slowly enough to reach thermodynamic equilibrium at each temperature. If it were lowered abruptly, the solid would freeze into a suboptimum state.

Fig. 2 illustrates the principle of SA. A modification of the estimate introduces a variation $\Delta\mathcal{F} = \mathcal{F}_{n+1} - \mathcal{F}_n$ of the cost function. For $\Delta\mathcal{F}$ negative the modified cost is lower than the previous cost, so the new estimate approaches the optimum and is accepted. If $\Delta\mathcal{F}$ is positive the modified estimate will not necessarily be rejected as is usually the case with conventional methods of local optimization. Such a worse estimate will be accepted according to a Boltzman probability distribution

$$p = \exp\left(-\Delta\mathcal{F}/kT\right) \tag{6}$$

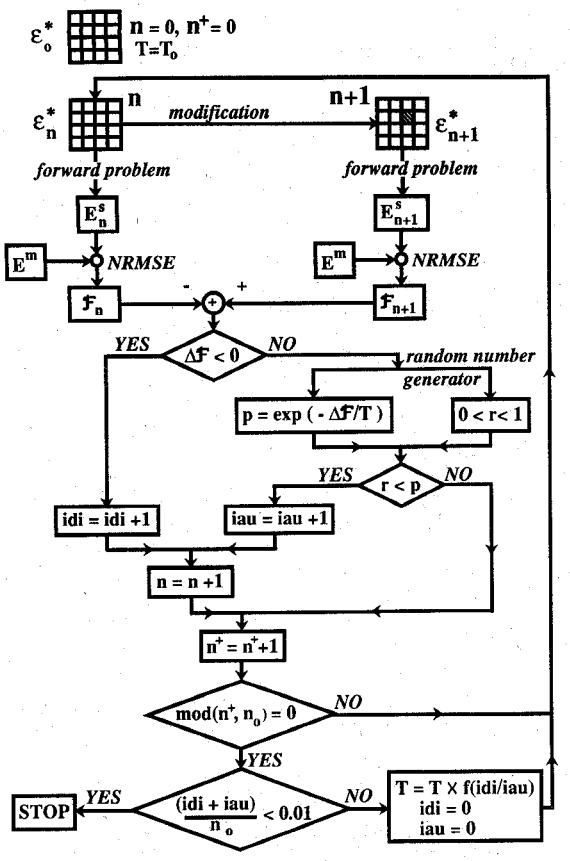

Fig. 3. The simulated annealing algorithm used for microwave tomography reconstruction. n^+ and n respectively represent the total number of iterations and the total number of accepted estimates. *idi* and *iau* are respectively the number of better and worse accepted estimates during the constant temperature interval of n_0 iterations.

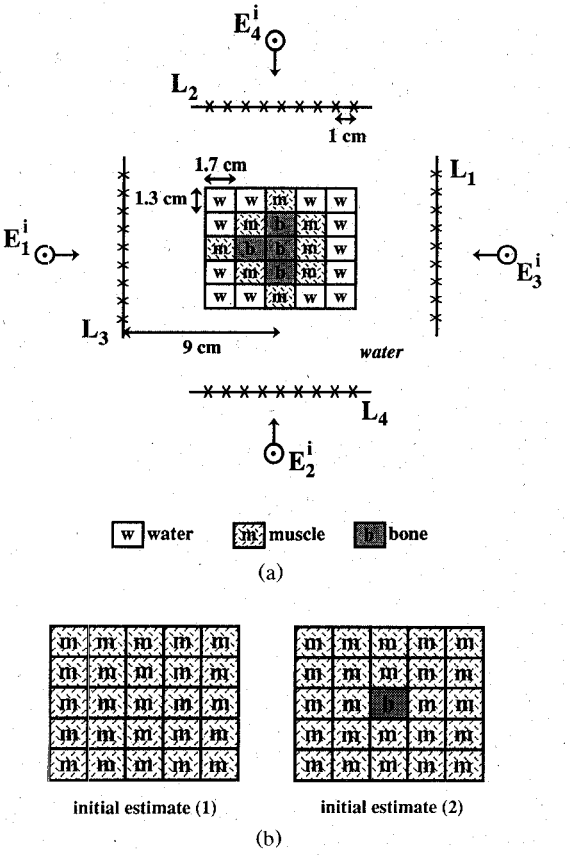

Fig. 4. (a) Geometry of the simulated experiment: four views are considered. The incident radiation is a plane wave propagating perpendicularly to the measurement line. (b) The two initial estimates.

where k is a constant, usually set to one and T a parameter called temperature. Random numbers between zero and one are generated for this purpose. For large T, p tends to one, so each worse estimate will be accepted. For small T, p tends to zero and only better estimates will do. The temperature is chosen high in the beginning and is lowered at equilibrium. In this context equilibrium is interpreted as the number of accepted worse estimates being, on average, equal to the number of better estimates. T equal to zero corresponds to a conventional method of local optimization or quenching, which often guides a system to a local minimum of the cost function. The virtue of SA and thus of introducing the probability (6) is that it gives the system a chance to escape from local minima.

C. Simulated Annealing: Application to Microwave Permittivity Reconstruction

Application of SA to microwave permittivity reconstruction requires the definition of a cost function, choice of an initial estimate for the complex permittivity distribution and of a way of modifying estimates, the definition of a temperature profile and of a criterion to stop the algorithm. For each estimate the scattered field E^s is calculated at discrete points on the line (forward problem) and compared to the corresponding measured or simulated scattering data E^m. We defined the cost function, which we want to minimize, as the Normalized Root Mean Square Error (NRMSE) between the scattering data and the calculated scattered field:

TABLE 1
VALUES OF THE RELATIVE PERMITTIVITY AND CONDUCTIVITY AT 2.45 GHz

2.45 GHz, 37° C	ϵ_r	$\sigma(\Omega m)^{-1}$
water	73.49	0.89
muscle	47.	2.16
bone	8.5	0.14

$$\mathcal{F} = \sqrt{\sum |E^s - E^m|^2} \Big/ \sqrt{\sum |E^m|^2}, \qquad (7)$$

where summations are taken over the measurement points and over the different views. It may be interesting to include in (7) terms expressing *a priori* information (smoothness, upper or lower bounds) or regularization terms [15]. We chose the initial estimate arbitrarily or according to available *a priori* information. For each iteration a grain $\Delta\epsilon^*$ was randomly added to or subtracted from the complex permittivity value of one cell. This cell may be picked at random, as we did in some preliminary examples [16], or sequentially which seems safer in the case of a large number of cells and which we

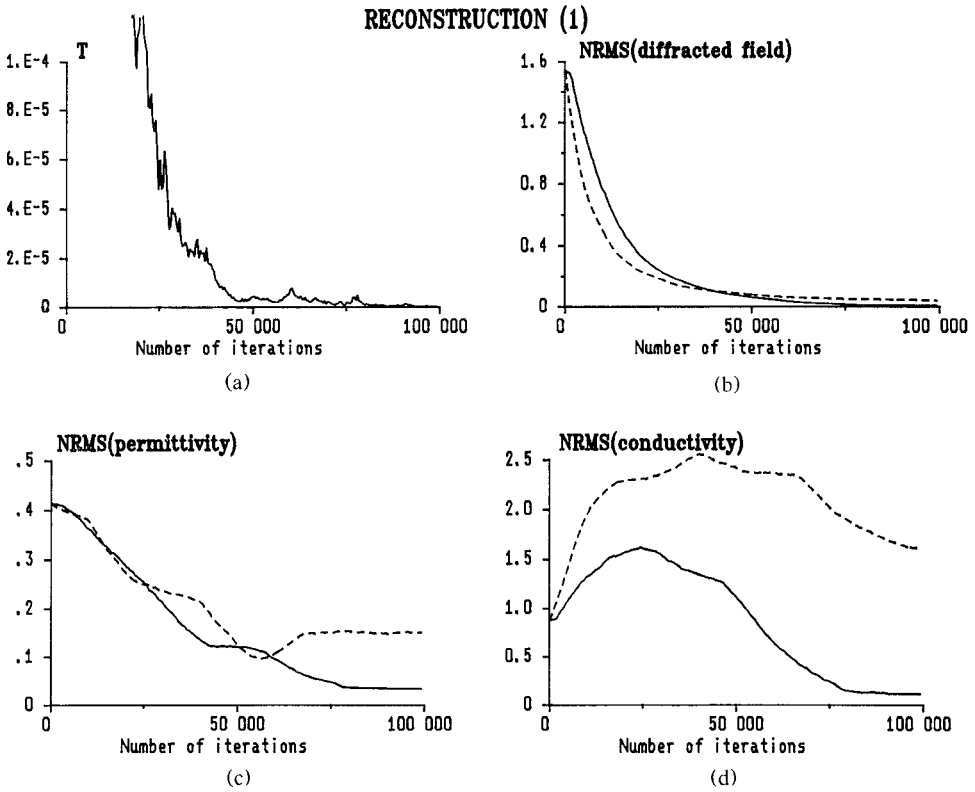

Fig. 5. Curves of the variation during the iterative process of: the annealing temperature (a), the cost function (b), the NRMS Error between the true and estimated relative permittivity (c) and between the true and estimated conductivity (d) for reconstructions with initial estimate (1). The solid lines correspond to SA and the dotted lines to quenching ($T = 0$).

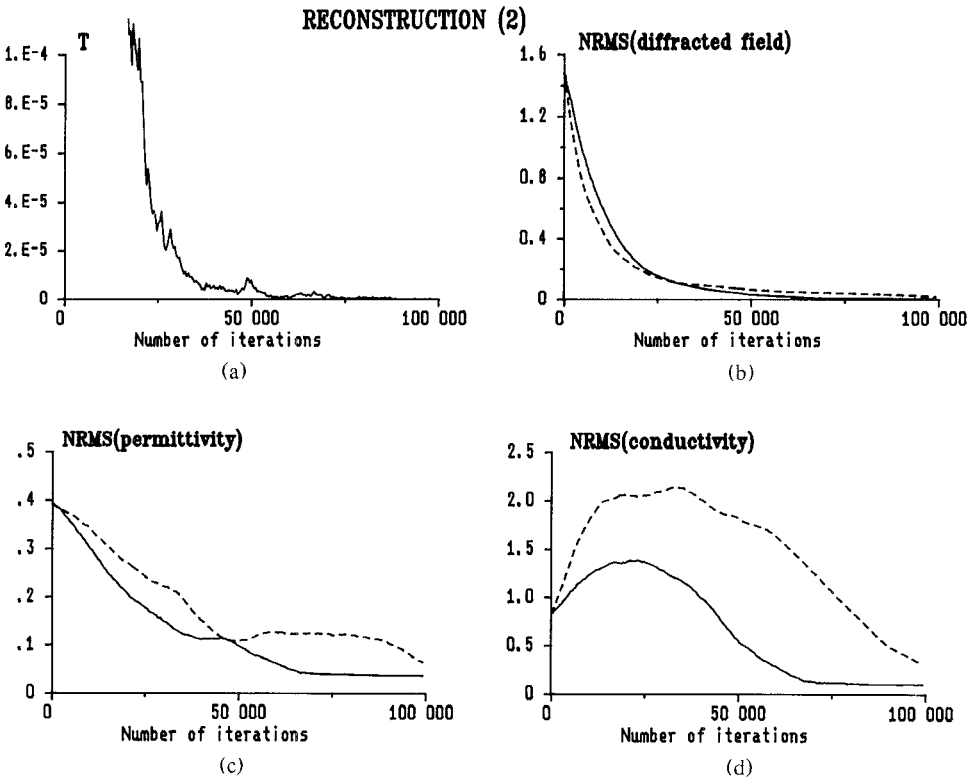

Fig. 6. Same as Fig. 5 for reconstructions with initial estimate (2).

chose for these examples. The value of the grain is chosen according to the dynamical range expected for the reconstruction i.e., small enough to satisfy the required precision and yet large enough to enhance the convergence speed. In order to accelerate the convergence we changed the temperature each time a fixed number of iterations was completed instead of waiting for equilibrium. At the end of a constant temperature interval, we decreased T if the system was close to equilibrium. If it was still far from equilibrium—i.e. the number of better estimates is significantly greater than the number of accepted worse ones—we raised T. In this way, annealing was maintained during the process. We stopped the algorithm when the ratio of the number of accepted estimates to the total number of iterations in a constant T interval fell below 1%. The process remains stationary for low values of this ratio, since the estimate is not significantly updated. Fig. 3 gives a schematic representation of SA applied to microwave tomography reconstruction.

The solution of the forward problem for each iteration requires an $N \times N$ matrix inversion as described earlier. This consumes excessive CPU time for large values of N. We were able to develop a fast inversion routine since only one cell, and so only one column in the matrix, is modified at a time (see Appendix).

IV. Numerical Simulations and Results

We will now present some results obtained with simulated noise-free data for the reconstruction of a simplified model of a human arm illuminated by a plane wave at 2.45 GHz. The arm is assumed to be infinitely long with a muscle and bone composition invariant along its length and immersed in water. Fig. 4(a) represents a cross-section discretized into 25 cells. Dielectric permittivity and conductivity at 2.45 GHz are listed in Table I. We calculated for this model, by means of a discretized version of the integral in (3), values of simulated measurements E^m at 36 points. Nine points are situated on a line L_k opposite to the source E_k^i and the line and source are rotated corresponding to four angles of incidence $k = 1 \cdots 4$ each separated by 90°. In our reconstruction algorithm the values E^m serve as a least squares reference since we minimize the cost function (7). Some prior knowledge of the solution was assumed to be available for the choice of the initial estimate. We performed reconstructions for two different initial estimates: 1) a homogeneous muscular estimate, and 2) a similar estimate containing a single bone cell in the middle (Fig. 4(b)). In both cases we have used SA, quenching ($T = 0$) and a numerical method based on a deterministic Newton–Kantorovich technique [12]. Throughout the reconstruction process we forced the permittivity and conductivity values to be positive.

Graphs comparing the convergence of SA (solid line) and of quenching (dotted line) are presented in Figs. 5 and 6 for the respective cases of the initial estimate. They show curves of the variation of the temperature (a); the cost function (b); the NRMSE between estimated and true values of the permittivity (c); and of the conductivity (d). The temperature, which we adapted every 25 scans of the object, rapidly decreases in the beginning of the process and then oscillates. Comparison of this annealing temperature scheme to schemes where T was slowly decreased revealed a faster convergence for the former. Curves $(b-d)$ show that SA leads to a more accurate solution than quenching. this phenomenon is more pronounced in the first case where less *a priori* information is available (Fig. 5). In the second case SA converges faster than quenching (Fig. 6). We also observe that the conductivity is never reconstructed as well as the relative permittivity. This is due to the relatively small values of $\sigma/\omega\epsilon_0$ with respect to ϵ_r. Nevertheless the algorithm manages to reconstruct the water and bone which have quite different dielectric properties to muscle.

A different way of presenting our reconstruction results are the complex permittivity distribution images. The value of the complex permittivity of each cell is represented by a rectangle whose width and height are proportional respectively to the dielectric permittivity and to the conductivity. Fig. 7 illustrates this representation for the model of the arm section. Figs. 8 and 9 give, for the respective reconstruction cases, the initial estimate (a); and results obtained with SA (b); with quenching (c); and with the Newton–Kantorovich method (d). We notice that SA seems to converge to a global minimum solution since the final results do not depend on the initial estimate.

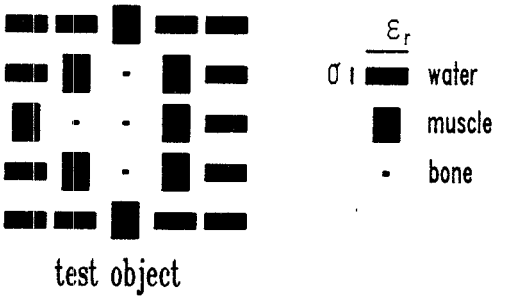

Fig. 7. Representation of the complex permittivity of the test object. The width and height of each rectangle are proportional respectively to ϵ_r and to σ.

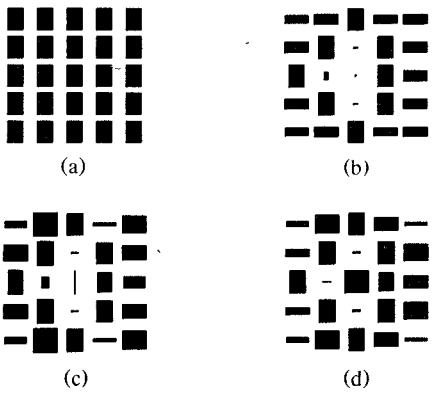

Fig. 8. Reconstructions of the test object with (a) initial estimate (1), obtained by the following methods: (b) SA; (c) quenching; (d) the Newton–Kantorovich method.

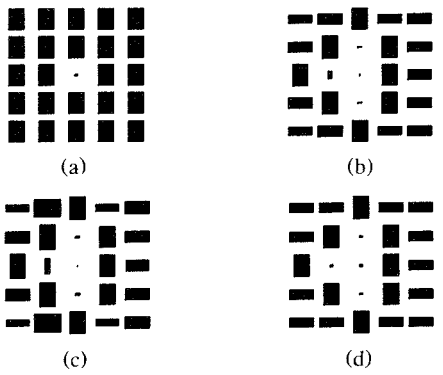

Fig. 9. Same as Fig. 8 for reconstructions with (a) initial estimate (2).

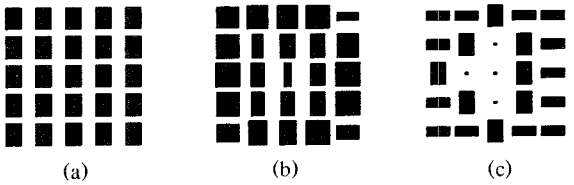

Fig. 10. Sequential application of SA and the Newton–Kantorovich method: (a) initial estimate for SA; (b) result after 25 000 iterations of SA and initial estimate for the Newton–Kantorovich method: (c) final result after eight iterations of the Newton–Kantorovich method.

Furthermore we conclude that SA can achieve satisfactory reconstructions in cases where deterministic methods fail to converge (Fig. 8(c)–(d)), i.e., when little prior knowledge is available or when the number of data is low. However, when the Newton-Kantorovich method converges, it does so in a much more efficient way with respect to the required computer time. By way of illustration 100 000 iterations of SA required a CPU time of one and a half hours on an IBM 9375 for our 5×5 cell object. We found that the time per iteration is proportional to $NM + N^2$ where N and M are respectively the number of cells and the number of measurements. The algorithm's behavior for larger objects is subject to further study but it seems clear that more iterations will be needed for convergence.

Finally we applied sequentially SA and the Newton–Kantorovich method to the case where the latter alone failed to converge. Fig. 10 shows an example where SA started from the homogeneous muscular estimate (a) and was stopped after 25 000 iterations. The corresponding result (b) served as an initial estimate for the Newton–Kantorovich method which reached the final result (c) after only eight iterations. We conclude that the suggested combination of methods still consumes considerable amounts of CPU time, although less than SA alone, but does exhibit convergence to an accurate solution when deterministic methods alone fail.

V. Conclusion

We have presented a preliminary study of the application of simulated annealing (SA) to complex permittivity reconstruction in microwave tomography. Reconstructions of a simplified model of a human arm obtained with simulated noise-free data have been presented for three different methods: SA, quenching and a Newton–Kantorovich method. These results are interesting since they show that SA can converge to an accurate solution in cases where the two deterministic methods fail. For this reason SA can be used to get closer to the final solution before applying a faster deterministic method. We admit that an infinite cylinder of arbitrary cross-sectional shape whose internal structure does not vary along its length is not an ideal approximation of the human arm, but we prefer first to explore the possibilities of two dimensional algorithms before examining the much more difficult three dimensional problem.

Much work still has to be done to fully evaluate the performances of SA for this type of application: we need to test the stability of the algorithm in the presence of noisy data, to introduce other cost functions to regularize the process and to try to accelerate the direct problem since the main disadvantage of SA still remains the amount of CPU time required.

Appendix

We derive here a fast inversion for a square matrix H written as

$$H = H_0 + \begin{pmatrix} 0 & \cdots & h_1 & \cdots & 0 \\ \vdots & & \vdots & & \vdots \\ 0 & \cdots & h_n & \cdots & 0 \end{pmatrix} \qquad \text{(A1)}$$

$$\uparrow$$

$$\text{column } l$$

where we assume that H_0^{-1} is already calculated. With the following notations,

$$h = \begin{pmatrix} h_1 \\ \vdots \\ h_n \end{pmatrix} \quad \text{and} \quad {}^t e_l = (0 \cdots 1 \cdots 0),$$

$$\uparrow$$

$$\text{column } l$$

(A1) also can be written as

$$H = H_0 + h\,{}^t e_l. \qquad \text{(A2)}$$

Multiplication by H^{-1} to the left and by H_0^{-1} to the right gives

$$H^{-1}HH_0^{-1} = H^{-1} + H^{-1}h\,{}^t e_l H_0^{-1}, \qquad \text{(A3)}$$

which leads to

$$H^{-1} = H_0^{-1} - (H^{-1}h)\,{}^t e_l H_0^{-1}, \qquad \text{(A4)}$$

or

$$H^{-1}h = H_0^{-1}h - (H^{-1}h)\,{}^t e_l H_0^{-1}h, \qquad \text{(A5)}$$

after multiplication by h. The scalar ${}^t e_l H_0^{-1}h$, which we note $(H_0^{-1}h)_l$, is the lth element of the column vector

$H_0^{-1}h$. From (A5) we deduce

$$H^{-1}h = \frac{1}{1+\left(H_0^{-1}h\right)_l} H_0^{-1}h, \qquad \text{(A6)}$$

and from (A6) and (A4):

$$H^{-1} = H_0^{-1} - \frac{1}{1+\left(H_0^{-1}h\right)_l}\left(H_0^{-1}h\right)\,{}^t e_l H_0^{-1}. \qquad \text{(A7)}$$

The expression $(H_0^{-1}h)\,{}^t e_l H_0^{-1}h$ represents a matrix with line i obtained by multiplying line l of H_0^{-1} by element i of $H_0^{-1}h$.

References

[1] J.Ch. Bolomey and Ch. Pichot, "Microwave tomography: from theory to practical imaging systems," *Int. J. Imaging Systems and Technology*, vol. 2, pp. 144–156, 1990.

[2] J.Ch. Bolomey, L. Joffre, and G. Peronnet, "On the possible use of microwave-active imaging for remote thermal sensing," *IEEE Trans. Microwave Theory Tech.*, vol. MTT-31, pp. 777–781, Sept. 1983.

[3] G. Gaboriaud, J.Ch. Bolomey, and Ch. Pichot, "Control of deep hyperthermia by means of active microwave imaging," in *Proc. 10th ESHO Conf.*, Amsterdam, The Netherlands, vol. 22, Sept. 1989.

[4] Ch. Pichot, L. Joffre, G. Peronnet, and J.Ch. Bolomey, "Active microwave imaging of inhomogeneous bodies," *IEEE Trans. Antennas Propagat.*, vol. AP-33, pp. 416–425, April 1985.

[5] W. Tabbara, B. Duchêne, Ch. Pichot, D. Lesselier, L. Chommeloux, and N. Joachimowicz, "Diffraction tomography: contribution to the analysis of some applications in microwaves and ultrasonics," *Inverse Problems*, pp. 305–331, Nov. 1988.

[6] M. Slaney, A. C. Kak and L. E. Larsen, "Limitations of imaging with first order diffraction tomography," *IEEE Trans. Microwave Theory Tech.*, vol. MTT-32, pp. 860–874, Aug. 1984.

[7] J.Ch. Bolomey, Ch. Pichot, and G. Gaboriaud, "Critical analysis of reconstruction algorithms devoted to a plane microwave camera for biomedical applications," in *Proc. URSI Int. Symp. Stockholm*, Sweden, August 1989, pp. 144–147.

[8] L. Joffre, M. S. Hawley, A. Broquetas, E. de los Reyes, M. Ferrando, and A. R. Elias-Fusté, "Medical imaging with a microwave tomographic scanner," *IEEE Trans. Biomed. Eng.*, vol. 37, pp. 303–312, Mar. 1990.

[9] S. Kirkpatrick, C. D. Gelatt, Jr., and M. P. Vecchi, "Optimization by simulated annealing," *Science*, vol. 220, pp. 671–680, 1983.

[10] W. E. Smith, R. G. Paxman, and H. H. Barrett, "Image reconstruction from coded data: I. Reconstruction algorithms and experimental results," *J. Opt. Soc. Am.*, vol. A 2, pp. 491–500, 1985.

[11] N. Joachimowicz, "Tomographie microonde: contribution à la reconstruction quantitative bidimensionnelle et tridimensionnelle," Ph.D. dissertation, University of Paris-VII, Mar. 1990.

[12] J. P. Hugonin, N. Joachimowicz, and Ch. Pichot, "Quantitative reconstruction of complex permittivity distributions by means of microwave tomography," *Inverse Methods in Action*, P. C. Sabatier, Ed., Berlin: Springer Verlag, 1990, pp. 302–311.

[13] J. H. Richmond, "Scattering by a dielectric cylinder of arbitrary cross section shape," *IEEE Trans. Antennas Propagat.*, vol. AP-13, pp. 334–341, May 1965.

[14] N. Metropolis, A. Rosenbluth, M. Rosenbluth, A. Teller, and E. Teller, "Equation of state calculations by fast computing machines," *J. Chem. Phys.*, vol. 21, pp. 1087–1092, 1953.

[15] H. Haneishi, T. Masuda, N. Ohyama, T. Honda, and J. Tsujiuchi, "Analysis of the cost function in simulated annealing for CT image reconstruction," *Appl. Optics*, vol. 29, pp. 259–265, 1990.

[16] A. Franchois, L. Garnero, Ch. Pichot, and J. P. Hugonin, "Application of the simulated annealing technique to microwave tomography: preliminary results," *Inverse Methods in Action*, P. C. Sabatier, Ed., Berlin: Springer Verlag, 1990, pp. 62–68.

Line Garnero received the Doctorat de troisème cycle and the Doctorat es Sciences degrees from the University of Paris XI (Orsay) in 1981 and 1987, respectively.

She joined the Institut d'Optique in Orsay in 1981. She is presently Chargé de Recherche at the Centre National de la Recherche Scientifique (CNRS). Her research interests include image reconstruction techniques for microwave and X-ray tomography, image processing, stochastic algorithms, and optical architectures.

Ann Franchois was born in Geel, Belgium, on November 8, 1964. She received the degree in electrical engineering from the University of Ghent, Belgium, in 1988 and the Diplôme d'Etudes Approfondies in optics from the University of Paris-Sud (Orsay) in 1989. She is presently working toward the Ph.D. degree at the University of Paris-Sud on the development of reconstruction methods in microwave tomography and its experimental verification.

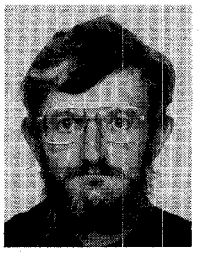

Jean-Paul Hugonin received the Doctorat d'Etat from the University of Paris XI (Orsay) in 1983. His research interests include image processing, digital photography and numerical theory of diffraction.

He has been Assistant Professor of physics at the University of Paris VI since 1974 and joined the Institut d'Optique in Orsay at the same time.

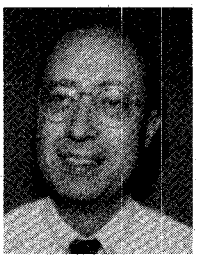

Christian Pichot was born in France, on March 6, 1951. He received the M.S. degree from the University of Nice, France, in 1974, the doctorat de Troisième Cycle and the Doctorat ès Sciences degrees from the University of Paris-XI (Orsay), France, in 1977 and 1982, respectively.

He joined the Groupe d'Electromagnétisme of the Laboratoire des Signaux et Systémes in 1978. He is presently a Chargé de Recherche at the Centre National de la Recherche Scientifique (C.N.R.S.). His research activities are concerned with scattering, direct and inverse and guided wave problems in inhomogeneous media. Since 1981 he is involved in microwave imaging for biomedical applications and since 1983 for civil engineering applications.

Dr. Pichot received the Microwave Prize of the European Microwave Conference in Nuremberg (F.R.G.) in 1983.

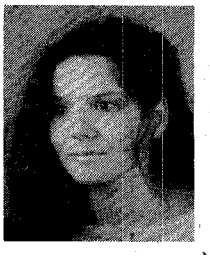

Nadine Joachimowicz was born in Paris, France, on December 12, 1963. She received the diplome d'Etudes Approfondies in physical methods for remote sensing in 1986 and the Ph.D. degree from the University of Paris-VII in 1990.

She is currently working on microwave imaging in the Groupe d'Electromagnétisme (C.N.R.S.-E.S.E.). Her fields of interest are direct and inverse problems in electromagnetism.